

# Improved Control of DFIG Systems under Unbalanced Voltage Dip for Torque Stability Using PI-Fuzzy Controller

Hai Nguyen-Thanh

HCMC University of Technical and Education, Vietnam  
Le Hong Phong High School for the Gifted, Ho Chi Minh City, Vietnam  
Email: {hai\_nguyenthanh2012, hoc\_vien}@yahoo.com.vn

**Abstract**—This paper introduces modified Stator Fed Oriented Control (SFOC) for Doubly Fed Induction Generator (DFIG) in wind turbines to reduce torque pulsation during unbalanced voltage; current waveforms are also improved with the decrease in harmonics. The proposed schemes apply multiple PI controllers with Fuzzy to obtain commanded rotor currents and also introduce extra commanded values for rotor current; Notch filters are also used to eliminate the second order harmonic components. The designed system consists of an induction generator with slip ring and back-to-back power electronic converters connected to both rotor and grid sides. The modifications are applied to the rotor side converter (RSC). Simulations in Matlab/Simulink illustrate the enhanced stability of torque response and improvement of current waveform. Comparisons of the simulation results with a traditional Stator Flux Oriented Control (SFOC) and a previously proposed modification for operation under unbalanced voltage are provided to evaluate the newly proposed methods in the paper.

**Index Terms**—DFIG, unbalanced voltage, PI controller, SFOC, fuzzy

## I. INTRODUCTION

Doubly fed induction generator (DFIG) has been widely used in wind farms for many years. The reasons for this popularity are the low cost of power electronic circuit needed to independently control of active and reactive powers delivered to the grid and the variable speed constant frequency operation [1], [2]. DFIG is the cheapest solution to on-shore wind farms when the whole systems are taken into consideration [3]. Therefore, more and more wind farms are connected to the grid and the penetration has been up to more than 50% in several countries [4]. However, the grids often experience problems such as unbalanced voltage dips, which causes an increase in winding temperature, pulsation of torque and power, oscillations of stator/rotor currents, and mechanical stress on the gear-box [5], [6]. Technical limitations for connected wind farms to maximize generator's output include voltage and reactive power

control, frequency control, and fault ride-through capabilities [4].

The stator voltage's magnitude is determined by the exchange of reactive power between generator and the grid while the phase difference is controlled by active power [4]. Therefore, power balance must be maintained on the grid. A voltage drop proportional to current and radial distance to the substations happens when a fault occurs. Due to the remote location of wind farms, the voltage difference may be well out of the limits and this could result in multiple disconnections on the wind farms [4].

The active power delivered to the grid by generator depends on the input mechanical power provided by the wind turbine. Therefore, a mismatch in power supply and demand on the distribution network could lead to a change in rotational energy stored in the generator. This will cause a decrease in frequency if the power supply is insufficient and an increase in frequency if the power supply is excessive. [4]

Fault ride-through capabilities are necessary for the wind farms to maintain connection to protect the network securities. During a voltage dip, DFIG will increase the demand of reactive power to a level that could cause further suppression of the grid voltage [4]. Wind farm disconnection as a result of this will cause a mismatch of power supply and demand and then results in frequency drop. Spinning power reserves have to be established for the grid if the generators are unable to ride through faults. Modification of control system is therefore necessary.

In addition to maintaining the connection to distribution network during voltage unbalance, generators need to keep providing sufficient powers with acceptable qualities, a modified SFOC based control method is proposed [6], using four command values of rotor current components so as  $i_{dr+}^{+*}, i_{qr+}^{+*}, i_{dr-}^{-*}, i_{qr-}^{-*}$  to achieve independent control of P and Q as well as constant torque, or constant active power, or balance stator current, or no oscillation of rotor current [7], [8].

This paper presents new SFOC based control schemes which use Torque Stability Controller (TSC) and PI controllers with Fuzzy to deduce  $i_{dr+}^{+*}, i_{qr+}^{+*}$  from active and reactive power errors. These PI-F controllers provide

simplicity to the control system and also increase the independence from the system with parameter's variations. The commanded values of  $i_{dr}^*$ ,  $i_{qr}^*$  are calculated from feedback quantities

## II. DYNAMIC MODEL OF DFIG SYSTEMS

This section discusses the control structure for vector control of grid-connected doubly fed induction generator. The control methods in [6], [9], [10] are based on Stator Flux Oriented Control, while the methods in [11] and this paper are based on SFOC with Torque Stability using PI-F Control.

Dynamic model of DFIG with balanced grid voltage in a generally rotating reference frame dq [2] is considered in this paper. Furthermore, positively and negatively rotating reference frames, which are denoted as dq+ and dq- respectively, are also used to develop control model for DFIG during unbalanced voltage dip. These reference frames are presented in the Fig. 1.

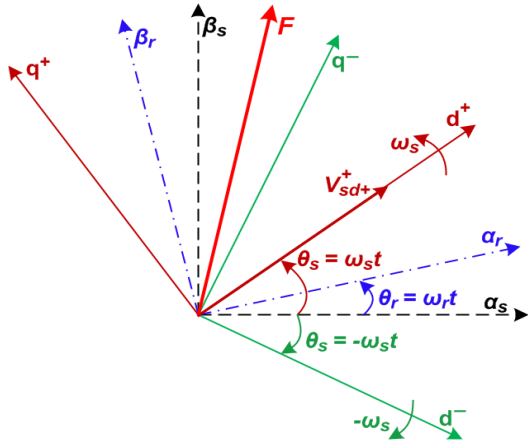


Figure 1. Relationships between  $(\alpha, \beta)_s$ ,  $(\alpha, \beta)_r$ , dq+ and dq- reference frames [6], [11].

$$I_{dq}^+ = I_{(\alpha\beta)_s} e^{-j\omega_s t} \quad I_{dq}^- = I_{(\alpha\beta)_s} e^{j\omega_s t} \quad (1.1)$$

$$I_{dq}^+ = I_{(\alpha\beta)_s} e^{-j2\omega_s t} \quad I_{dq}^- = I_{(\alpha\beta)_s} e^{j2\omega_s t} \quad (1.2)$$

$$I_{dqr}^+ = I_{dqr+}^+ + I_{dqr-}^+ = I_{dqr+}^+ + I_{dqr-}^- e^{-j2\omega_s t} \quad (1.3)$$

In a Stator Flux Oriented Control (SFOC) reference frame, where the d axis is attached the stator flux space vector, the following characteristics are obtained:

$$\psi_{ds} = |\psi_s| = L_m i_{ms} \quad (2.1)$$

$$\psi_{qs} = 0 \quad (2.2)$$

The stator voltage equations of DFIG in a generally rotating reference frame dq, as shown in equations (3) and (4)

$$v_{ds} = R_s i_{ds} - \omega_s \psi_{qs} + \frac{d\psi_{ds}}{dt} \quad (3)$$

$$v_{qs} = R_s i_{qs} + \omega_s \psi_{ds} + \frac{d\psi_{qs}}{dt} \quad (4)$$

Therefore, the equations for active and reactive powers in the stator flux reference frame are shown in equation (5.1) and (5.2)

$$P_s = \frac{3}{2}(v_{ds} i_{ds} + v_{qs} i_{qs}) = \frac{3}{2} v_{qs} i_{qs} = -\frac{3}{2} |\psi_s| \frac{L_m}{L_s} i_{qr} \quad (5.1)$$

$$Q_s = \frac{3}{2}(v_{qs} i_{ds} - v_{ds} i_{qs}) = \frac{3}{2} v_{qs} i_{ds} = \frac{3}{2} |\psi_s| \frac{L_m}{L_s} \left( \frac{|\psi_s|}{\omega_s L_m} - i_{dr} \right) \quad (5.2)$$

The equations above have shown that independent control of P and Q can be achieved by controlling  $i_{dr}$  and  $i_{qr}$  in SFOC.

When in unbalanced voltage, the equations for active and reactive powers in the stator are shown in [6] and [9].

$$P_s = P_{s0} + P_{s\_sin2} \sin(2\omega_s t) + P_{s\_cos2} \cos(2\omega_s t) \quad (6.1)$$

$$Q_s = Q_{s0} + Q_{s\_sin2} \sin(2\omega_s t) + Q_{s\_cos2} \cos(2\omega_s t) \quad (6.2)$$

with

$$\begin{pmatrix} P_{s0} \\ Q_{s0} \\ P_{s\_sin2} \\ Q_{s\_sin2} \\ P_{s\_cos2} \\ Q_{s\_cos2} \end{pmatrix} = \frac{3}{2\omega_s L_s} \begin{pmatrix} 0 & 0 & 0 & 0 \\ v_{qs+}^+ & -v_{ds+}^+ & -v_{qs-}^- & v_{ds-}^- \\ -v_{qs-}^- & -v_{ds-}^- & -v_{qs+}^+ & -v_{ds+}^+ \\ -v_{ds-}^- & v_{qs-}^- & v_{ds+}^+ & -v_{qs+}^+ \\ 0 & 0 & 0 & 0 \\ 0 & 0 & 0 & 0 \end{pmatrix} \times \begin{pmatrix} v_{qs+}^+ \\ v_{ds+}^+ \\ v_{qs-}^- \\ v_{ds-}^- \end{pmatrix} \quad (7)$$

$$+ \frac{3L_m}{2L_s} \begin{pmatrix} v_{ds+}^+ & v_{qs+}^+ & v_{ds-}^- & v_{qs-}^- \\ v_{qs+}^+ & -v_{ds+}^+ & v_{qs-}^- & -v_{ds-}^- \\ v_{ds-}^- & -v_{ds-}^- & -v_{qs+}^+ & v_{ds+}^+ \\ v_{ds-}^- & v_{qs-}^- & v_{ds+}^+ & v_{qs+}^+ \\ -v_{ds-}^- & -v_{qs-}^- & v_{ds+}^+ & v_{qs+}^+ \\ v_{qs-}^- & -v_{ds-}^- & v_{qs+}^+ & -v_{ds+}^+ \end{pmatrix} \times \begin{pmatrix} i_{dr+}^+ \\ i_{qr+}^+ \\ i_{dr-}^- \\ i_{qr-}^- \end{pmatrix}$$

The total power imported from the rotor shaft equals to the sum of the power output from the equivalent voltage source  $j\omega_s \psi_s$  and  $j(\omega_s - \omega_r) \psi_r$ .

$$P_e = -\frac{3}{2} \text{Re}[j\omega_s \psi_s^+ \hat{I}_s^+ + j(\omega_s - \omega_r) \psi_r^+ \hat{I}_r^+] \quad (8.1)$$

$$= \frac{3}{2} \omega_r \text{Re}[j\psi_s^+ \hat{I}_r^+]$$

$$P_e = P_{e0} + P_{e\_sin2} + P_{e\_cos2} \quad (8.2)$$

where

$$\begin{bmatrix} P_{e0} \\ P_{e\_sin2} \\ P_{e\_cos2} \end{bmatrix} = \frac{3L_m \omega_r}{2L_s} \begin{bmatrix} -\psi_{sq+}^+ & \psi_{sd+}^+ & -\psi_{sq-}^- & \psi_{sd-}^- \\ \psi_{sd-}^- & \psi_{sq-}^- & -\psi_{sd+}^+ & -\psi_{sq+}^+ \\ -\psi_{sq-}^- & \psi_{sd-}^- & -\psi_{sq+}^+ & \psi_{sd+}^+ \end{bmatrix} \begin{bmatrix} I_{rd+}^+ \\ I_{rq+}^+ \\ I_{rd-}^- \\ I_{rq-}^- \end{bmatrix} \quad (9)$$

The electromagnetic torque of the DFIG is calculated as



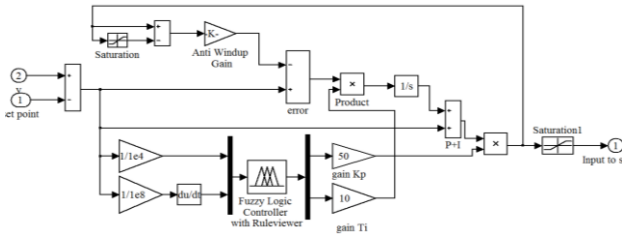


Figure 5. PI-Fuzzy Controller. [12]

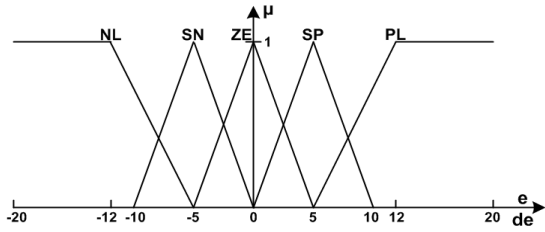


Figure 6. Membership functions of two inputs of fuzzy block.

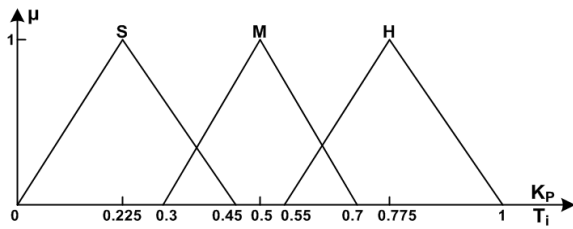


Figure 7. Membership functions of two outputs of fuzzy block

The fuzzy rules for parameters of PI-FUZZY controllers are presented in Table I and Table II. The rules are developed by trial and error. LN, SN, ZE, SP, and LP represents large negative, small negative, zero, small positive, large positive. S, M, H are for small, medium, high. The triangular membership functions of inputs and outputs of PI-Fuzzy controller are shown in Fig. 6 and Fig. 7.

TABLE I. RULE BASE OF  $K_p$  [11]

$K_p$	de/dt				
	LN	SN	ZE	SP	LP
e	LN	H	H	H	H
	SN	H	M	M	H
	ZE	M	S	S	M
	SP	M	M	M	H
	LP	M	H	H	H

TABLE II. RULE BASE OF  $T_i$  [11]

$T_i$	de/dt				
	LN	SN	ZE	SP	LP
e	LN	H	H	H	H
	SN	H	M	M	H
	ZE	H	M	S	M
	SP	H	M	M	H
	LP	H	H	H	H

#### IV. SIMULATION RESULTS

We carry out the simulations of the proposed control methods for the 2.3MW grid-connected DFIG with the parameters given in Table III. The commanded values of P and Q are altered every 50s, with the reference value of P

changing from 1.5MW to 2.0MW while that of Q from 1.2MVAR to 800kVAR. The grid voltages are balanced until the 60<sup>th</sup> second, at which point one of the phase voltages is reduced by 10%. The voltages are then balanced again from the 80<sup>th</sup> second (Fig. 8). The proposed control methods are for the variable speed and constant frequency of DFIG; without loss of generality, the rotor speed is super-synchronous and remains at a fixed value of 1600rpm. The wind speed's variation is shown in Fig. 9.

TABLE III. PARAMETERS OF THE 2.3MW DFIG

Parameter	Symbol	Value
Stator inductance	$L_s$	159.2 ( $\mu H$ )
Rotor inductance	$L_r$	159.2 ( $\mu H$ )
Magnetic inductance	$L_m$	5.096 ( $mH$ )
Stator resistance	$R_s$	4 ( $m\Omega$ )
Rotor resistance	$R_r$	4 ( $m\Omega$ )
Number of pole pairs	$p$	2
Frequency of the electric system	$\omega_s$	100 $\pi$ ( $rad/s$ )
Inertia	$J$	93.22 ( $kg.m^2$ )
Inertia of Rotor	$J_{rot}$	4.17 $\times 10^6$ ( $kg.m^2$ )

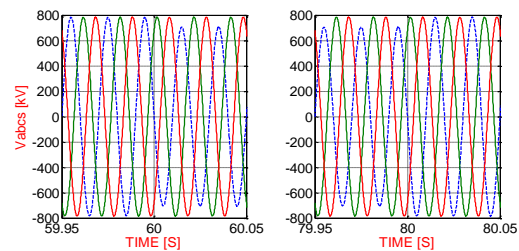


Figure 8. The grid voltages are balanced until the 60<sup>th</sup> second, one of the phase voltages is reduced by 10%, then they are balanced again from the 80<sup>th</sup> second

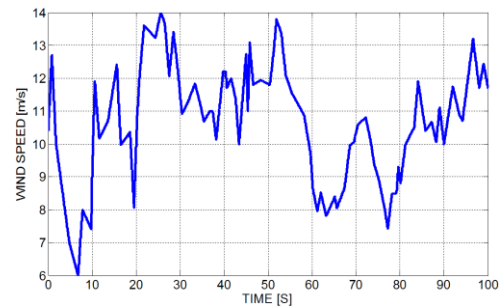


Figure 9. Random variation of the wind speed.

The simulations are based on the assumption that the DFIG has operated in a stable condition for a long time after starting and grid synchronization. Fig. 10-Fig. 19 present the responses of active power, reactive power, stator current, rotor current and torque.

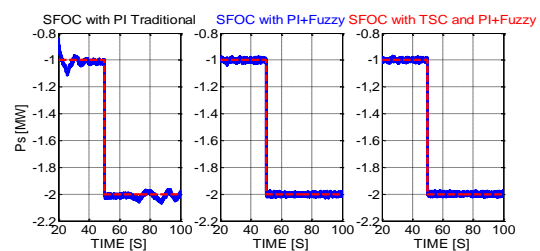


Figure 10. Active output power of DFIG

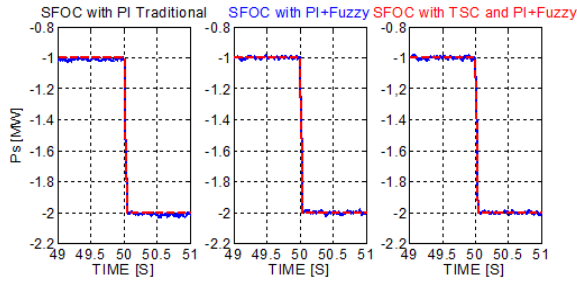


Figure 11. Active power during transient state.

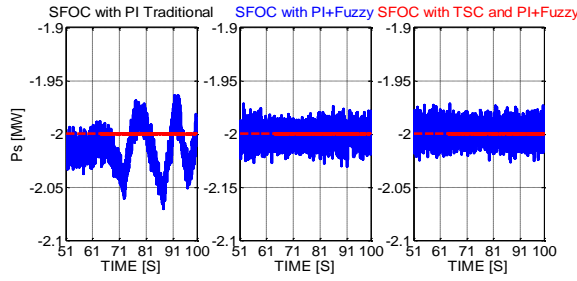


Figure 12. Active power during unbalanced voltage.

The red lines in the figures above are the commanded values of P and Q. For active and reactive power, we observe the average values over a period of time. However, instantaneous values are collected for stator current, rotor current and torque.

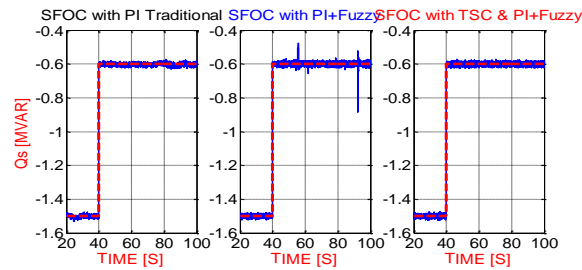


Figure 13. Reactive output power of DFIG.

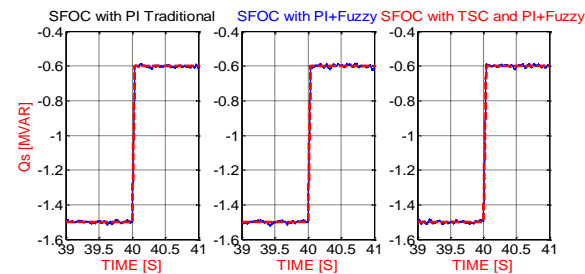


Figure 14. Reactive power during transient state.

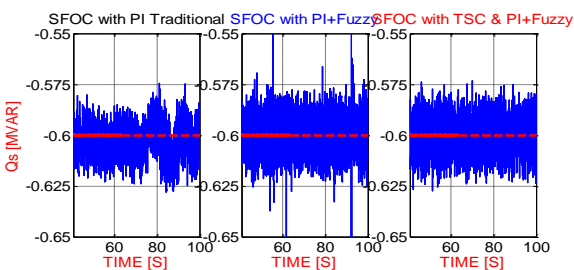


Figure 15. Reactive power during unbalanced voltage.

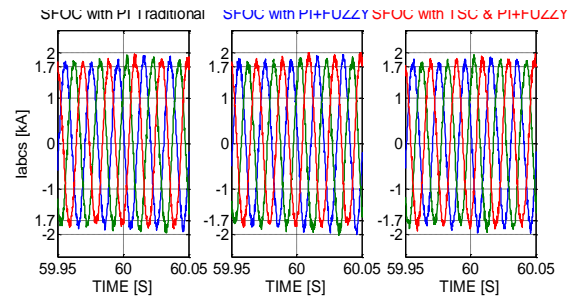


Figure 16. Stator current before and during unbalanced voltage.

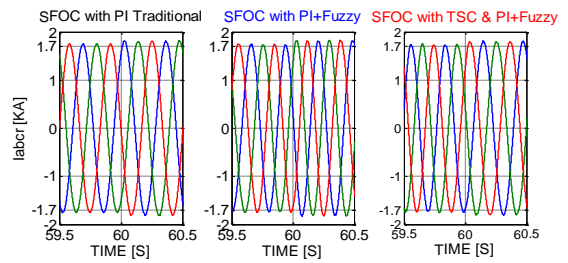


Figure 17. Rotor current before and during unbalanced voltage.

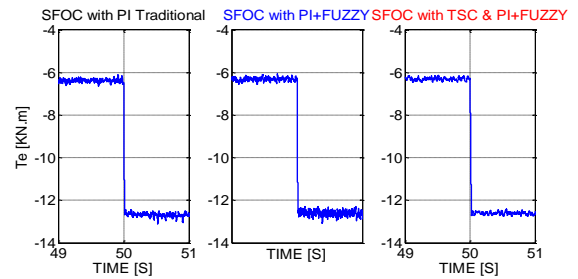


Figure 18. Generator torque during transient state and unbalanced voltage.

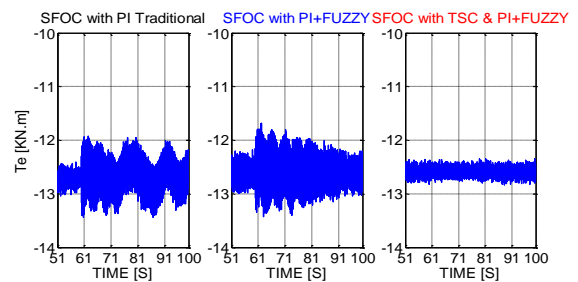
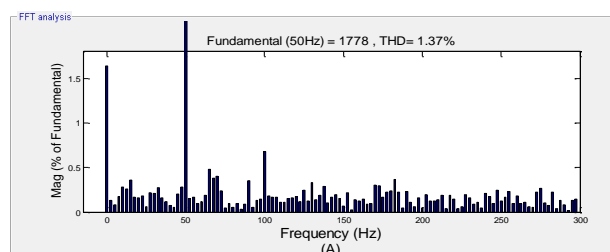


Figure 19. Generator torque during unbalanced voltage.

Fig. 20 and Fig. 21 show harmonics analyses of the currents. In each figure, there are three sub-figures for the responses obtained by traditional SFOC (A), previously proposed method by PI+Fuzzy (B), and previously proposed method by TSC and PI+Fuzzy (C).



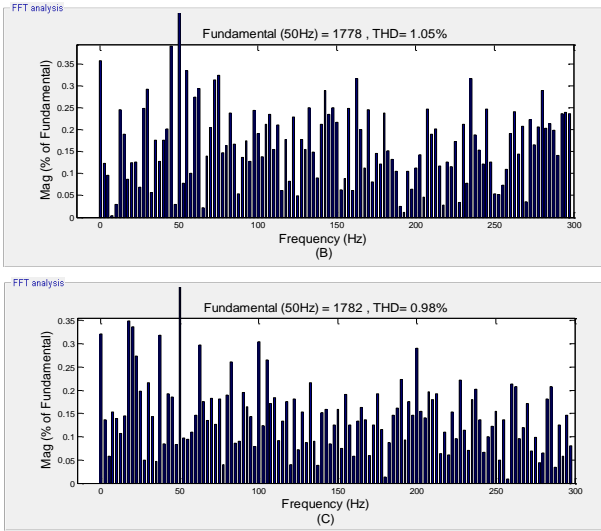


Figure 20. THD's Stator current balanced voltage. (Traditional SFOC (A), previously proposed method by PI+Fuzzy (B), and previously proposed method by TSC and PI+Fuzzy (C))

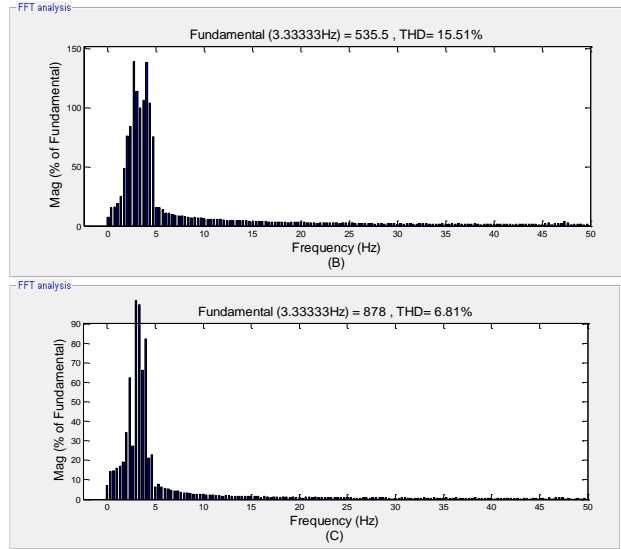


Figure 22. THD's Rotor current balanced voltage. (Traditional SFOC (A), previously proposed method by PI+Fuzzy (B), and previously proposed method by TSC and PI+Fuzzy (C))

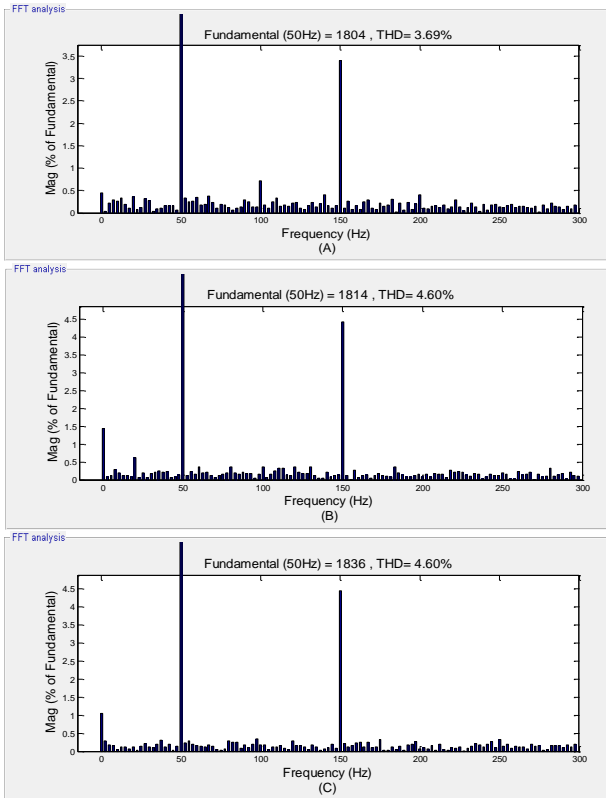


Figure 21. THD's Stator current unbalanced voltage. (Traditional SFOC (A), previously proposed method by PI+Fuzzy (B), and previously proposed method by TSC and PI+Fuzzy (C))

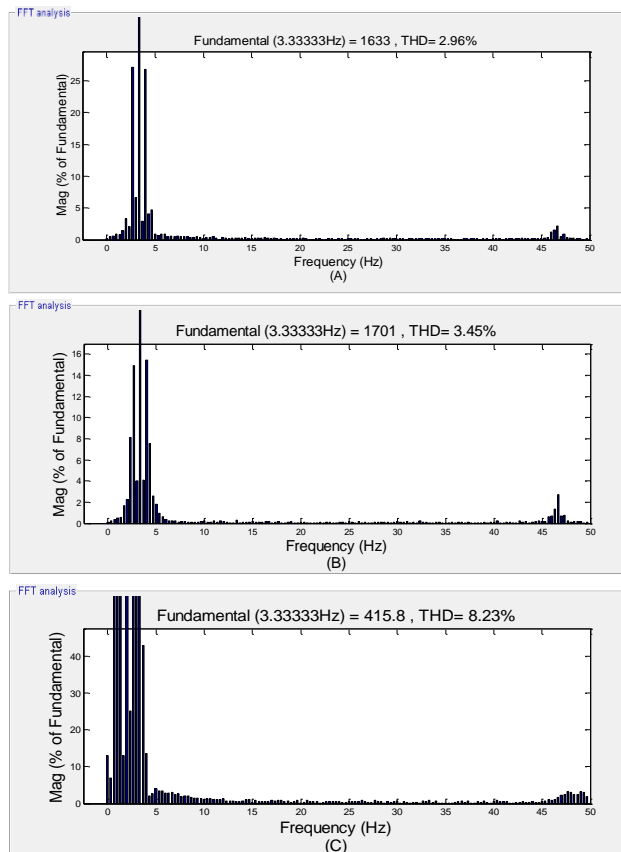


Figure 23. THD's Stator current unbalanced voltage. (Traditional SFOC (A), previously proposed method by PI+Fuzzy (B), and previously proposed method by TSC and PI+Fuzzy (C))

## V. DISCUSSION

Fig. 10, Fig. 11 and Fig. 12 show that the proposed methods have insignificant steady-state errors in active power responses during balanced voltage, especially when compared to the steady-state errors of the traditional SFOC method. During unbalanced voltage,

this gives power responses with less pulsation than the other two methods and also with smaller steady-state errors, as shown in Fig. 10, Fig. 11 and Fig. 12.

The responses of reactive powers are quite similar to each other for the three methods during the transient state and the steady state in balanced voltage. The results in Fig. 13, Fig. 14 and Fig. 15 also show better reactive power for the two proposed methods which are less oscillated.

The waveforms of stator current and rotor current in the three modified control methods are less distorted when unbalanced voltage happens as shown in Fig. 16 and Fig. 17.

The performance of generator torque is much better for the proposed control scheme in this paper during unbalanced voltage as shown in Fig. 18 and Fig. 19. These methods give less torque pulsation compared to the other two methods with SFOC; even modification for coping with voltage unbalance is included. The reduction of torque's variation helps to decrease the mechanical stresses on wind turbine systems.

Harmonic analysis of rotor current has shown little difference in the frequency spectrum of the three control methods (the SFOC PI traditionally, the SFOC PI+Fuzzy and SFOC TSC & PI+Fuzzy in this paper) during the balanced voltage. Rotor frequency is about 3.33 Hz when the rotor speed is 1600 rpm. The energy contents in higher order harmonics are quite small during the balance as shown in Fig. 22 and Fig. 23.

Harmonic contents of stator current during balanced voltage are quite good for the three control schemes above as shown in Fig. 20 and Fig. 21. The THD's is almost the same in these figures. Table IV shows the comparison of THD in the three methods on operating conditions, balanced, and unbalanced voltages.

TABLE IV. THD COMPARISON FOR STATOR & ROTOR CURRENT

THD		PI	PI-F	TSC and PI-F
<b>Balanced grid Voltage</b>	$I_r$	6.81	15.51	8.2
	( $f=3.3\text{Hz}$ )	0%	127.7%	20.4%
	$I_s$	0.98	1.05	1.37
	( $f=50\text{Hz}$ )	0%	7.1%	39.8%
<b>Unbalanced grid Voltage</b>	$I_r$	8.23	3.45	2.96
	( $f=3.3\text{Hz}$ )	0%	<b>-58.1%</b>	<b>-64%</b>
	$I_s$	4.6	4.6	3.96
	( $f=50\text{Hz}$ )	0%	<b>0%</b>	<b>-13.9%</b>

$$Deviation = \frac{THD - THD_{Traditional\ SFOC}}{THD_{Traditional\ SFOC}} (\%)$$

Total harmonic distortion on the rotor currents of the two new control schemes has been significantly reduced during the unbalanced voltage (64% for SFOC using TSC with PI+Fuzzy and 58.1% for SFOC with PI+Fuzzy). For stator current, it is 13.9% for SFOC using TSC with PI+Fuzzy and 0% for SFOC with PI+Fuzzy when compared with the THD in the traditional SFOC with the super-synchronous rotor speed. All of the THD's stator and rotor currents increase during the unbalanced voltage.

Although the controlling target of the proposed methods in this paper is the constant generator's torque to

reduce mechanical stresses, the obtained results are satisfactory not only for the torque but also for stator and rotor current harmonics as well as active and reactive powers.

## VI. CONCLUSION

The new SVOC-based control methods, which use TSC and PI controllers with Fuzzy to deduce rotor current's commanded positive components in positively rotating reference frame and two extra commanded values for rotor current's negative components in negatively rotating reference frame, are proposed in the paper. Verifications of the control schemes by Matlab/Simulink during balanced and unbalanced voltage of 10% in one phase, steady and transient states, have also been presented. The results have showed significantly reduced torque pulsation. Improved responses of active and reactive powers are also observed for the proposed ones.

The results are also compared with the ones obtained from simulation of traditional SFOC PI and modified SFOC using PI+Fuzzy.

In the future, simulations of the proposed control structures with other expressions of the rotor current commands to achieve three targets suggested in [6] and [7] (constant active power, no oscillation of rotor current, and balanced stator current) should also be done. Experimental verifications should also be implemented.

## APPENDIX NOMENCLATURE

$v_s, v_r$	Stator, rotor voltage vectors.
$i_s, i_r$	Stator, rotor current vectors.
$\psi_s, \psi_r$	Stator, rotor flux vectors.
$\omega_s$	Stator angular frequency.
$\omega$	Rotor speed.
$P_s, Q_s$	Stator output active and reactive power.
$L_m$	Mutual inductance.
$L_{\sigma s}, L_{\sigma r}$	Stator, rotor leakage inductances.
$L_s, L_r$	Stator, rotor self inductances.
$R_s, R_r$	Stator, rotor resistance
$\theta_r$	Rotor angle
$\theta_s$	Stator flux angle in SFOC

### Superscripts

+, -	Positively, negatively (dq) rotating reference frames.
*	Reference value for controllers.

### Subscripts

$\alpha, \beta$	Stationary $\alpha$ - $\beta$ axis.
$\alpha_r, \beta_r$	Rotor $\alpha_r$ - $\beta_r$ axis.
$d, q$	Rotating $d$ - $q$ axis.
$s, r$	Stator, rotor.
+, -	Positive, negative components.

## REFERENCES

- [1] T. Ackermann, *Wind Power in Power Systems*, USA: John Wiley and Sons, 2003.
- [2] W. Leonhard, *Control of Electric Drives*, 3<sup>rd</sup> ed., USA: Springer-Verlag, 2001.
- [3] J. Wenske, "Special report direct drives and drive-train development trends," in *Wind Energy Report Germany 2011*, Siemens Press Picture, 2011.
- [4] M. I. Alegría, J. Andreu, L. J. Martí, P. Ibanez, L. J. Villate, and H. Camblong, "Connection requirement for wind farms: A survey on technical requirements and regulation," *Renewable and Sustainable Energy Review*, vol. 11, no. 8, pp. 1858-1872, 2007.
- [5] E. Muljadi, D. Yildirim, T. Batan, and C. P. Butterfield, "Understand the unbalanced-voltage problem in wind turbine generation," in *Proc. IEEE Industry Application Conference*, Phoenix, USA, 1999, pp. 1359-1365.
- [6] L. Xu and Y. Wang, "Dynamic modeling and control of DFIG based wind turbines under unbalanced network conditions," *IEEE Transactions of Power Systems*, vol. 22, no. 1, pp. 314-323, 2007.
- [7] Y. K. Hu, J. B. He, and Z. Rende, "Modeling and control of wind-turbine used DFIG under network fault conditions," in *Proc. The Eight International Conference on Electrical Machines and Systems ICEMS 2005*, Nanjing, China, 2005, vol. 2, pp. 986-991.
- [8] J. B. Hu, Y. K. He, X. Lie, and W. B. Williams, "Improve control of DFIG systems during network unbalance using PI-R current regulators," *IEEE Transactions on Industrial Electronics*, vol. 56, no. 2, pp. 439-451, 2009.
- [9] T. Pham-Dinh, A. N. Nguyen, and H. Nguyen-Thanh, "Improving stability for independent power control of wind turbine doubly fed induction generator with SFOC and DPC during grid unbalance," in *Proc. The 10<sup>th</sup> International Power and Energy Conference IPEC 2012*, Ho Chi Minh City, Vietnam, 2012, pp. 155-160.
- [10] J. B. Hu and Y. K. He, "Modelling and enhance control of DFIG under unbalanced grid voltage conditions," *Electric Power Systems Research*, vol. 79, no. 2, pp. 272-281, 2009.
- [11] T. Pham-Dinh, H. Nguyen-Thanh, H. Uchida, and N. G. M. Thao, "Comparison between modifications of SFOC and PDC in control of grid-connected doubly fed induction generator under unbalanced voltage dip," in *Proc. SICE Annual Conference 2013*, Nagoya, Japan, 2013, pp. 2581-2588.
- [12] T. Pham-Dinh and H. Nguyen-Thanh, "Improving stability for independent power control of wind-turbine doubly fed induction generator during grid unbalance with PI-Fuzzy controller," *Journal of the Japan Society of Applied Electromagnetics and Mechanics*, vol. 21, no. 3, pp 425-429, 2013.



**Hai Nguyen-Thanh**, He received his B.S. and M.S. degrees from Hochiminh City University of Technology, Vietnam, in 2000 and 2012, respectively. He is currently a Ph.D. student at HCMC University of Technical and Education, Vietnam. He is a member of IACSIT. His research interest is wind power generation, intelligent control and renewable energy system.